

Antimicrobial Activity of Biosynthesized Selenium Nanoparticles using *Pseudomonas Aeruginosa*

Laila A. Elshikiby¹, Zakaria A.M. Baka¹ and Mohamed M. El-Zahed^{*1}

¹Department of Botany and Microbiology, Faculty of Science, Damietta University, New Damietta city, Egypt.

Received: 20 May 2025 /Accepted: 20 June 2025

*Corresponding author's E-mail: Mohamed.marzouq91@du.edu.eg

Abstract

The current study used *Pseudomonas aeruginosa* isolated from clinical specimens to provide a simple and cost-effective approach for biosynthesizing selenium nanoparticles (SeNPs). Vitek 2 was used to confirm the species-level identification of the chosen bacterial isolate after it was recognized traditionally. The biosynthesized SeNPs were verified and described using a variety of tests, including TEM, FT-IR, zeta analyses, and UV-Vis spectroscopy. At 330-370 nm, the adsorption peaks for SeNPs were recorded. The presence of proteins acting as binding and supporting components during synthesis was verified by the FT-IR spectra. The substantial negative surface charge of -17.6 mV contributes to its stability. TEM shows the diameters of SeNPs in the 83-91 nm range. SeNPs had strong antimicrobial activity against *Bacillus cereus*, *Staphylococcus aureus*, *Proteus mirabilis*, *Pseudomonas aeruginosa*, and *Candida albicans* in a dose-dependent manner. The MICs of SeNPs against *B. cereus*, *S. aureus*, *P. aeruginosa*, *P. mirabilis*, and *C. albicans* were 40, 70, 110, 150, and 150 µg/mL, respectively. This study offers safe, effective, and promising nanoparticles as an alternative for treating some pathogenic microbes in both humans and animals.

Keywords: *Pseudomonas aeruginosa*, selenium nanoparticles, characterization, antimicrobial activity

Introduction

Antimicrobial resistance (AMR) poses a significant risk to public health worldwide; in 2019; bacterial AMR was linked to about 5 million deaths (Murray et al., 2022). Combating AMR necessitates a comprehensive and integrated strategy that includes improved infection prevention and control measures, enhanced global policies and funding, AMR

surveillance, improved understanding of mechanisms and drivers at the individual and population levels, and the development of innovative antimicrobial therapeutic strategies. Extreme poverty is made worse in low- and middle-income countries (LMICs) by the effects of AMR-related illness or mortality. If the issue is not resolved, LMICs are predicted to lose more than 5% of their economy by 2050 as a result of lost revenue from indirect healthcare costs (O'Neill, 2016).

The effectiveness of almost all known

antibiotics is impacted by a variety of bacterial resistance mechanisms, such as decreased membrane permeability, the use of efflux pumps, enzyme modification or antibiotic degradation, alteration of antibiotic targets, and adaptive mechanisms like biofilm formation. The majority of AMR usually happens 0–6 months after antibiotic exposure (Poku et al., 2023), highlighting the enormous issue of AMR, even if the timing of resistance development may range across various antibiotic-bacteria combinations.

Escherichia coli, *Staphylococcus aureus*, *Klebsiella pneumoniae*, *Streptococcus pneumoniae*, *Acinetobacter baumannii*, and *P. aeruginosa* were the six main causes (73%) of AMR-associated mortality in 2019, according to the 2022 Global Burden of Disease research (Miller & Arias, 2024). One separate group of pathogens, ESKAPEE, which includes *Enterococcus* species, *S. aureus*, *K. pneumoniae*, *A. baumannii*, *P. aeruginosa*, *Enterobacter* species, and *E. coli* is known to cause drug-resistant infections in hospital settings. These infections have a wide range of intrinsic or acquired resistance mechanisms that allow them to live or flourish in healthcare settings.

Pseudomonas is a genus of Gram-negative bacteria. It is a member of the class Gammaproteobacteria and the family Pseudomonadaceae. While not all strains of this bacterial species are known to cause infections (Xiao et al., 2024), some species, such as *Pseudomonas aeruginosa*, *P. stutzeri*, and *P. putida*, are known to do so. The bacterium can usually survive in a healthy body, and since it doesn't damage anyone, healthy people frequently carry the bacteria without realizing it. Sometimes, mild infections might develop, resulting in problems like hot tub rash or swimmer's ear. *Pseudomonas* infections can be severe or even fatal for people with compromised immune systems or those who are already unwell. There are more than 300 *Pseudomonas* species (Parte et al., 2020). Opportunistic infections—infections that arise in persons with compromised immune systems because of medical illnesses or drugs that weaken the immune system—are caused by the majority of organisms that cause disease in humans. Some strains linked to opportunistic infections are *P. aeruginosa*, *P. putida*, *P. fluorescens*, and *P. stutzeri*. Although the entire body can be impacted by *pseudomonas*, the

infection and its symptoms are more likely to occur in specific organs and parts of the body. These include the urinary tract, ear canal, skin injuries, and lungs. Studies have shown that up to 10% of *Pseudomonas* infections are resistant to antibiotics. They are hard to cure since they may avoid drugs and survive. Resistance mechanisms can be acquired through horizontal gene transfer (acquiring aminoglycoside-modifying enzymes and β -lactamases) or mutations that overexpress efflux pumps or β -lactamases or decrease expression or change target sites and porins. External stimuli, such as antibiotic exposure, activate adaptive resistance mechanisms, which then become inactive when the stimulus is removed (Kunz Coyne et al., 2022).

Currently, improvements in technology, such as nanotechnology, and nanomaterials are often utilized separately or in combination with antibiotics as promising, effective antimicrobial agents for solving AMR concerns. Nanotechnology is a modern science subject that studies and affects the properties of matter at the nanoscale. Nanoparticles (NPs) range in size from 1 to 100 nm and exhibit chemical stability, antifungal properties, low toxicity, and low pathogen resistance (Manimaran et al., 2023). NPs, including Ag, Cu, Au, Fe, and Se, play important roles in agriculture, food, the environment, and nanomedicine (Saqib et al., 2022). NPs can be manufactured in a variety of ways, including physical, chemical, and biological techniques. The increasing cost and toxicity of physical and chemical techniques has led to an increase in green synthesis of NPs. It employs biological substances like plant extracts, fungus, and bacteria. This environmentally benign technology provides a long-term alternative to existing chemical and physical synthesis methods by decreasing the usage of harmful chemicals and boosting the biocompatibility of NPs (Khan et al., 2022). Green synthesis methods can be divided into two categories: top-down and bottom-up approaches. These approaches differ in terms of nanoparticle formation and control over size, shape, and characteristics.

Bacteria are recommended for NPs syntheses because they require minimal conditions, are easy to purify, and produce high yield. As a result, bacteria have become the most studied microorganism, earning the label of "the factory of nanomaterials. Bacteria can operate as a biocatalyst for inorganic material synthesis, a

bio-scaffold for mineralization, or an active component in nanoparticle formation (Iqtedar et al., 2019). Bacteria can produce nanomaterials in broth media during an incubation period, either as extracellular or intracellular. This characteristic makes the biosynthesis of NPs using bacteria a feasible, versatile, and acceptable method for large-scale manufacturing.

Inorganic NPs of metals such as Ag, Au, Ce, Fe, Se, Ti, and Zn hold an important place among NPs due to their distinct bioactivities in nanoforms. Se is a necessary trace element. It is integrated into selenoproteins as selenocysteine, which forms the majority of the active core of their enzymatic activity. Many seleno proteins function as oxidoreductases, regulating the physiological redox balance. Se has a restricted therapeutic window and extremely fragile toxicity margins, but Se nanoparticles (SeNPs) have far lower toxicity. SeNPs have been studied in a variety of oxidative stress and inflammation-mediated illnesses, including arthritis, cancer, diabetes, and nephropathy, for possible therapeutic benefits. SeNPs make an appealing carrier platform for transporting diverse medicines to the site of action (Khurana et al., 2019). NPs' antimicrobial mechanisms include membrane and bacterial cell wall destruction, protein and internal component damage, ion release, DNA damage, and oxidative stress (Besinis et al., 2014).

NPs have a wide range of antibacterial actions, which means that bacteria are unlikely to develop resistance to them (Huh & Kwon, 2011). Thus, the current study aimed to biosynthesize SeNPs using *Pseudomonas aeruginosa* isolate and evaluate their antimicrobial action.

Materials and methods

Sample collection

In April and May 2024, 22 samples (12 females and 10 males) were obtained from various private clinics and medical analytical laboratories in New Damietta City, Kafr Elbattikh, and Faraskour (Damietta Governorate, Egypt, 31.4°N 31.72°E). These samples included urine, stool, and surface swab samples. The samples were processed using the previously outlined procedures by Santiago-

Rodriguez et al. (2015) and Zboromyrska & Vila (2016).

Isolation and identification of bacterial isolates

The spread plate method was used to isolate drug-resistant pathogenic bacteria on a blood agar basis (Oxoid Ltd., England) supplemented with 2 mg/l ceftazidime (MCKC) and 5% (wt/v) defibrinated, sterile sheep blood (Youri et al., 2007). At 37°C, each plate was incubated for 24 hours. The hemolytic reaction caused by microorganisms was then noted. For 48 hours, each bacterial colony from a different bacterial isolate was transferred and subcultured on Cystine Lactose Electrolyte Deficient (CLED, Oxoid Ltd., England) agar plates. Then, colonial morphological characteristics and color change of colonies and media were recorded. The bacterial isolates were characterized and identified according to Bergey's Manual of Systematic Bacteriology (Yahr & Parsek, 2006). The morphological and cultural characteristics included colony shape, Gram staining, and endospore staining, and the identification was done in a systematic manner as follows: Colonial characters (size, form, pigment production, elevation, surface, edge, color, and opacity) were recorded. Microscopic examination included shape, size, Gram stain, acid fast stain, and endospore formation. The species-level was identified using the Vitek 2 (BioMerieux, Marcy-l'Étoile, France) (Moore et al., 1981).

Antibiotic sensitivity test (AST)

The AST of bacterial isolates was evaluated using the disc diffusion technique (CLSI, 2000a). 50 µL of each bacterial suspension (0.5 MacFarland Standard, 1.5×10^8 CFU/mL) was separately added to Mueller-Hinton agar (MHA, Oxoid Ltd., England) flasks, which were then placed into sterile Petri dishes. Vanomycin (30 µg/mL), amoxicillin/clavulanate (20/10 µg/mL), ampicillin (30 µg/mL), cefotaxime (30 µg/mL), ceftazidime (30 µg/mL), chloramphenicol (30 µg/mL), doxycycline (30 µg/mL), levofloxacin (5 µg/mL), nalidixic acid (30 µg/mL) and amoxycillin/clavulanate (20/10 µg/mL) were among the antibiotic discs from different classes that were aseptically applied after solidification. The diameter of the zones of

inhibition (ZOI) was measured and recorded in millimeters after a 24-hour incubation period at 37°C.

Biosynthesis of selenium nanoparticles

The selected bacterial isolate was grown in nutrient broth medium overnight at 37°C. After the incubation, the bacterial cells were discarded and the bacterial metabolites were collected using centrifugation of bacterial cultures at 4000 rpm for 20 minutes. The obtained bacterial supernatant was filtered using a 0.22 µm syringe filter (Millex GV, Millipore). Sodium selenite solution (1 mM) was prepared, mixed with the selected bacterial isolate supernatant at a ratio of 1:1 (v/v%), and shaken well (150 rpm) at 37°C for 24 hours (Mohamed & El-Zahed, 2024).

Characterization of selenium nanoparticles

A double-beam spectrum UV–Vis spectrophotometer V-760 (JASCO, UK) and Fourier transform infrared spectroscopy (FT-IR, FT/IR-4100 type A) were two of the methods used to examine the biosynthesized SeNPs. Transmission electron microscopy (TEM, JEOL JEM-2100, Japan) and zeta potential measurements (Malvern Zetasizer Nano-ZS90, Malvern, UK) were used for additional analysis.

Antimicrobial activity of selenium nanoparticles using agar well diffusion method

Different concentrations (50, 150, and 300 µg/mL) of SeNPs were evaluated for their antibacterial and anticandidal activities against *Bacillus cereus*, *Staphylococcus aureus*, *Proteus mirabilis*, *P. aeruginosa*, and *Candida albicans* using the agar well diffusion method, in accordance with the Clinical and Laboratory Standards Institute (CLSI, 2017). Nutrient agar and yeast extract peptone agar media were prepared and inoculated with 0.5 MacFarland standard ($1-2 \times 10^8$ CFU/mL) from the microbial strains. Ampicillin and miconazole were used as control antibiotics. 100 µL from each antibacterial agent was added to wells, and the inoculated plates were incubated at 37°C or 30°C for bacteria or yeast, respectively. Zones of inhibition were measured in mm.

Minimal inhibitory concentration (MIC)

The MICs of SeNPs were assessed using the broth microdilution method in compliance with CLSI guidelines (CLSI, 2000b; 2008). Standard antibiotics and serial solutions (0-150 µg/mL) from SeNPs were made and examined. The test microorganisms were cultivated for 24 hours at 37°C for yeast and 30°C for bacteria. Following the incubation period, a spectrophotometer was used to measure the turbidity of the microbial growth at 600 nm in relation to the growth control.

Minimum microbicidal concentration (MMC)

Using the pour plate approach, each MIC microbiological flask was inoculated into Mueller-Hinton agar plates, and the bacteria or yeast were then incubated at 37°C or 30°C, respectively. The total number of microbial colonies was expressed in colony-forming units per milliliter (CFU/mL) (Owuama, 2017).

Antioxidant activity of selenium nanoparticles

According to Turan et al. (2025), the antioxidant activities of SeNPs were examined using the in vitro DPPH radical scavenging technique. At 517 nm, the maximum absorbance of DPPH radical solutions takes place. Ethanol was used to reduce the absorbance of the control sample to 1.5 ± 0.5 after a 1 mM DPPH radical solution was prepared. The results were compared using the established antioxidant ascorbic acid (vitamin C). Different dosages of the DPPH radical solution (10–110 µg/mL) were given to the samples and standards separately. After the samples were incubated for 30 minutes at 25°C, the absorbance values were calculated. Absorbance at 517 nm decreases when a sample is able to scavenge DPPH free radicals. The percentage (%) of inhibition of DPPH was determined using the formula $\% = (A_{\text{control}} - A_{\text{compound}} / A_{\text{control}}) \times 100$, where A_{control} represents the absorbance in the absence of the compound and A_{compound} represents the absorbance in the presence of the compound.

Statistical analysis

SPSS version 18 software was used to perform statistical analysis of the data. The analysis was conducted using one-way analysis of variance (ANOVA), and each experimental value is displayed as the mean \pm standard deviation

(SD). A significance threshold of $p < 0.05$ was set. Every experiment was run in triplicate.

Results

Isolation, purification, and characterization of P. aeruginosa isolates

Sixteen Gram-negative, rod-shaped, positive citrate and glucose-fermenting bacteria that did not ferment lactose or form spores were identified from the 24-hour-developed resistant bacterial colonies and chosen for subculturing on CLED agar plates. When these bacteria were separated on CLED agar plates, eight of the isolates showed a yellow hue, five showed no color, and three showed a pale pink tint. On CLED agar plates, colonies that were smooth, pale, or colorless were chosen and allowed to grow (Atlas & Synder, 2011). Translucent blue colonies were chosen and purified after 48 hours, and the Vitek 2 was used to identify the species. This revealed the existence of two *P. aeruginosa* isolates encoded with BSF2 and BSF6 (Table 1, Figure 1). The two isolates of *P. aeruginosa* were examined for SeNPs production.

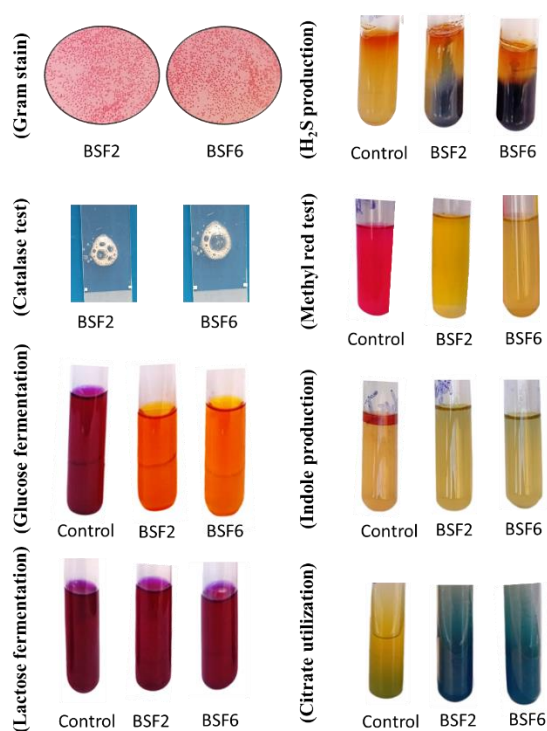


Figure 1. Some representative biochemical tests of the bacterial isolates.

Table 1. Biochemical tests for *P. aeruginosa* isolates.

Biochemical test	BSF2	BSF6
Citrate utilization	+	+
Catalase	+	+
Oxidase	+	+
Indole production	-	-
Methyl red	-	-
Voges-Proskauer	-	+
Urease	+	+
Nitrate reduction	+	-
H ₂ S production	+	+
Lactose fermentation	-	-
Glucose fermentation	±	±

*+ = Positive; - = Negative; ± = Intermediate reaction.

AST investigations

Table 2 shows that the BSF6 strain is more resistant to all tested antibiotics than the BSF2 strain. According to the findings, the isolates of *P. aeruginosa* have a 100% resistance rate to ampicillin, cefotaxime, ceftazidime, doxycycline, and vancomycin. Amoxicillin/clavulanate, chloramphenicol, levofloxacin, and nalidixic acid revealed antibacterial action against *P. aeruginosa* BSF2. The outcomes showed that the *P. aeruginosa* isolates exhibited multidrug resistance.

Table 2. Patterns of antibiotic resistance and sensitivity in *P. aeruginosa* isolates.

Antibiotic	Concentration (µg/ml)	Antibiotics susceptibility	
		BSF2	BSF6
Amoxicillin/clavulanate	20/10	+	-
Ampicillin	30	-	-
Cefotaxime	30	-	-
Ceftazidime	30	-	-
Chloramphenicol	30	+	-
Doxycycline	30	-	-
Levofloxacin	5	+	-
Nalidixic acid	30	+	-
Vancomycin	30	-	-

Biosynthesis and characterization of SeNPs

The color of the reaction mixture varies from pale yellow at the beginning of the experiment to red at the end of the incubation time, which is used to evaluate the production of SeNPs by the *P. aeruginosa* isolates (Figure 2). In the control studies, the color of the sample remained unchanged. *P. aeruginosa* BSF6 isolate showed the highest production rate within 24 hours when compared to the other isolate, BSF2, according to the UV-Vis spectrometric assay used to confirm the

formation of SeNPs. When SeNPs were produced utilizing the cell-free metabolites of various isolates of *P. aeruginosa*, absorbance maxima between 330 and 370 nm were found.

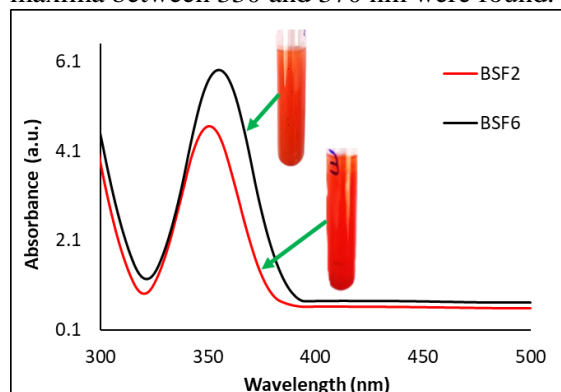


Figure 2. Color change and UV-Vis spectroscopy analysis of the biosynthesized SeNPs using *P. aeruginosa* isolates; BSF2 and BSF6.

FT-IR, TEM, and zeta potential studies were used to analyze the biosynthesized SeNPs that *P. aeruginosa* BSF6 generated. The FT-IR spectra of the bacterial crude protein and the protein attached to the surface of SeNPs showed distinct changes in peak location and shape (Figure 3), suggesting that the secondary structure of the protein underwent changes after NPs formation. FT-IR data have shown that contact with SeNPs has affected the secondary structure of proteins. It is possible to attribute the broad peak at 3633.23 cm^{-1} to the hydroxyl (-OH) group. The C-H vibration is credited with the peak at 1700.91 cm^{-1} . The bands at 1447.31 cm^{-1} might be caused by the C-O stretching mode. The amide II band, which appears at bands $3116.4\text{--}2498.33\text{ cm}^{-1}$, is a combination of N-H in-plane bending and C-N stretching, while the amide I band is mostly a C=O stretching mode. Se vibration (C-Se) is responsible for 549.61 cm^{-1} emergence.

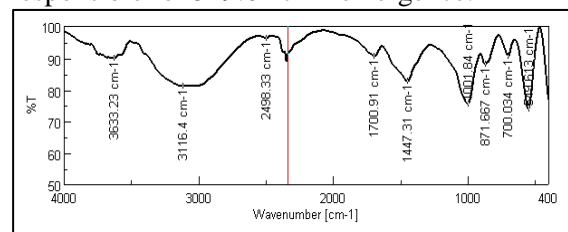


Figure 3. FT-IR of the biosynthesized SeNPs.

One crucial measure of the stability of the NPs' colloidal dispersion is still the zeta potential. The measurement of an effective electric charge on NPs' surface is called the zeta potential. Higher electrostatic repulsion between NPs causes the NPs with a larger zeta potential to be

more stable. The biosynthesized SeNPs' negative charge (-17.6 mV) was shown by the Zeta potential measurements, as illustrated in Figure 4.

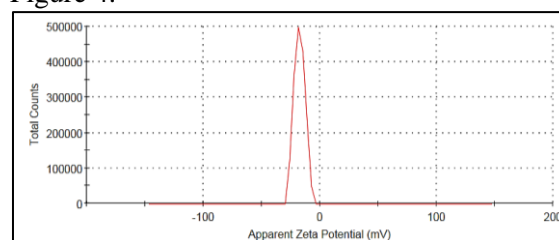


Figure 4. Zeta potential analysis of SeNPs.

An essential tool for assessing and studying the size and shape of NPs is the TEM investigation. The TEM micrograph of SeNPs demonstrated their uniform distribution, spherical shape, and absence of aggregation (Figure 5). The size of SeNPs ranged from 83.45 to 91.64 nm.

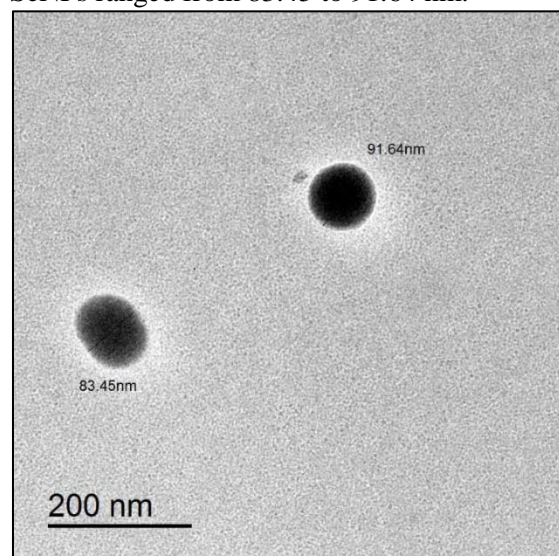


Figure 5. TEM of SeNPs with scale bar = 200 nm.

Antimicrobial activity of the biosynthesized SeNPs

SeNPs were bio-produced utilizing *P. aeruginosa* BSF6, and their antibacterial efficacy against several Gram-positive and Gram-negative bacteria as well as yeast was examined. SeNPs' antibacterial activity was evaluated using the agar well diffusion technique, MIC, and MBC assays, in contrast to the conventional antibiotics ampicillin and miconazole. The inhibition zones formed by the $150\text{ }\mu\text{g/ml}$ SeNPs were 20 ± 0.06 and $12\pm 0.03\text{ mm}$ against Gram-positive *B. cereus* and *S. aureus*, and 10 ± 0.18 and $9\pm 0.16\text{ mm}$ against Gram-negative *P. aeruginosa* and *P. mirabilis*, respectively (Table 2). SeNPs demonstrated

better antibacterial and anticandidal properties than the medical standards miconazole and ampicillin. Additionally, it was mentioned that

Table 2. Agar well diffusion of SeNPs against the tested microbes.

Antimicrobial agents	Concentration, $\mu\text{g/mL}$	Inhibition zone in mm (mean \pm SD)				
		Gram-negative bacteria		Gram-positive bacteria		Yeast
		<i>P. aeruginosa</i>	<i>P. mirabilis</i>	<i>B. cereus</i>	<i>S. aureus</i>	<i>C. albicans</i>
SeNPs	50	-ve	-ve	13 \pm 0.21	8 \pm 0.06	10 \pm 0.14
	100	7 \pm 0.14	6 \pm 0.23	17 \pm 0.14	10 \pm 0.06	12 \pm 0.06
	150	10 \pm 0.16	9 \pm 0.18	20 \pm 0.06	12 \pm 0.03	14 \pm 0.14
Ampicillin	50	-ve	-ve	15 \pm 0	-ve	-
	100	-ve	-ve	20 \pm 0	-ve	-
	150	-ve	-ve	22 \pm 0	6 \pm 0	-
Miconazole	50	-	-	-	-	8 \pm 0
	100	-	-	-	-	10 \pm 0
	150	-	-	-	-	12 \pm 0

The antimicrobial properties of the synthesized SeNPs were also evaluated using MIC and MBC (Figure 6). The MICs of SeNPs against *B. cereus*, *S. aureus*, *P. aeruginosa*, *P. mirabilis*, and *C. albicans* were 50, 70, 120, 150, and 50 $\mu\text{g/mL}$, respectively. The MBC values were 60, 80, 120, and 150 $\mu\text{g/mL}$ against *B. cereus*, *S. aureus*, *P. aeruginosa*, and *P. mirabilis*, respectively. This indicated that the biosynthesized SeNPs were more effective against Gram-positive than Gram-negative bacteria. SeNPs showed dose-dependent antimicrobial activity against all test microbes, which increased by increasing their concentration. *P. mirabilis* followed by *P. aeruginosa* showed low sensitive behavior to SeNPs. To demonstrate a complete bacterial inhibition, high concentrations of SeNPs (150 $\mu\text{g/mL}$) were needed.

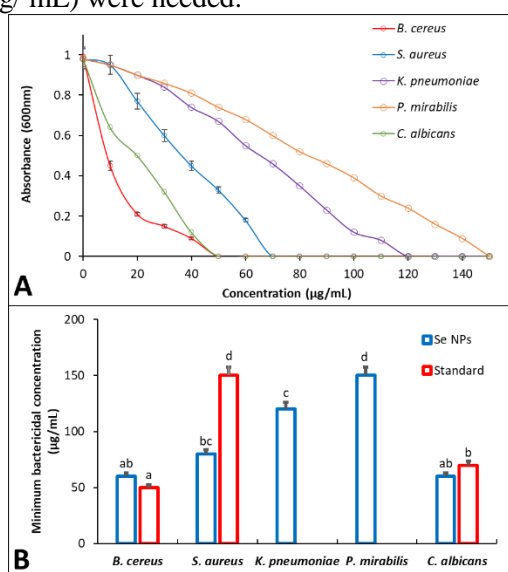


Figure 6. The minimum inhibition concentrations and minimum microbicidal concentrations of SeNPs compared to standards; miconazole and ampicillin.

SeNPs work better against bacteria that are Gram-positive than those that are Gram-negative.

Antioxidant activity

The antioxidant qualities of the biosynthesized SeNPs were evaluated using the in vitro DPPH radical scavenging approach (Figure 7). The experiment's results showed that the radical scavenging ratio increased as the concentrations in the measured range increased and that SeNPs had a concentration-dependent scavenging effect. SeNPs have a 68.2% DPPH radical scavenging activity. At all doses, ascorbic acid, a common antioxidant, outperformed the SeNPs in this investigation.

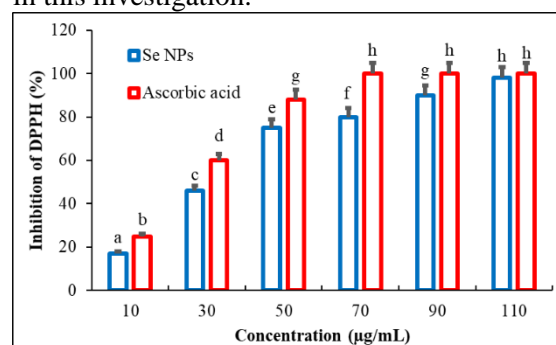


Figure 7. DPPH scavenging activity of SeNPs.

Discussion

An international health emergency is the rise in antibiotic resistance. The battle against microbes was believed to be won. Through a variety of processes, either inherent to the organism or acquired from another, microorganisms can become resistant to novel antimicrobials (Reygaert, 2018). *Pseudomonas* bacteria is one of the most serious bacterial infections due to causing several diseases for the whole part of the body, and the most

dangerous problem is the resistance to antibacterial agents. Although certain types of antibacterial medications, such as ampicillin and ciprofloxacin, are extreme irritants and potentially bactericidal, many studies have found antibacterial resistance in *Pseudomonas* bacteria (Garg et al., 1999). This study seeks to identify an alternative green strategy to bacterial infection concerns, namely *Pseudomonas* resistance to current commercial medications. According to several studies, *P. aeruginosa* cases of β -lactam antibiotic resistance have been discovered (Gniadkowski, 2001; Subedi et al., 2018). Using common biochemical methods, two strains of *P. aeruginosa* that are resistant to drugs were successfully isolated and identified in the current study. The CLSI criteria and an *in vitro* method were employed to assess these bacteria's resistance to different antimicrobial medications. This project also aims to find a different green way to address the issue of bacterial resistance, notably *P. aeruginosa* resistance to the commercial drugs that are currently on the market.

Certain nano-metals and nano-oxides, including Fe, ZnO, Cu, Ag, Mn, Se, Au, and Al, have been found to exhibit antibacterial properties. Nano-metals are primarily synthesized using several physical and chemical techniques. However, as well as toxicity, high reactivity, and instability, drawbacks have been established, including the usage of expensive precursors and the creation of hazardous wastes (Baka et al., 2019; El-Zahed et al., 2023; Fayed et al., 2023). The biological synthesis of nanomaterials is therefore becoming more and more necessary. Bacteria are good instruments for nano-metal manufacturing because they are diverse and adaptable to harsh environmental conditions (Wang et al., 2017). For example, *P. aeruginosa* was found to synthesize AuNPs (Husseiny et al., 2007) and *K. pneumoniae* was also reported for SeNPs biosynthesis (Fesharaki et al., 2010).

To validate the synthesis of NPs, first, qualitatively change the color of the culture media from yellow to red brick color, which is caused by the conversion of selenite to selenium as an element; over time, the sodium selenite in the culture medium changes color to red (Abbas et al., 2021). This implies that selenite has been reduced to elemental Se, and the characteristic red hue produced indicates the resonance of the surface Plasmon of SeNPs.

The SeNPs biosynthesis was confirmed by an absorbance peak that ranged from 330 to 370 nm. Several research studies observed various absorbance peaks for SeNPs. For example, the maximum light absorption was at 294 nm for SeNPs, as reported by Tabibi et al. (2020). In a different study, a team of researchers used microorganisms isolated from several regions of Saudi Arabia to create SeNPs; the chosen strain had an absorption peak at 290 nm (El-Deeb et al., 2018). The manufacture of SeNPs using the bacteria *Ralstonia eutropha* was the subject of another investigation in 2015. This artificial NPs's absorption peak is visible at 270 nm (Srivastava & Mukhopadhyay, 2015). Numerous investigations demonstrate that synthesized SeNPs have a resonance peak at 200–300 nm. Nevertheless, this absorption peak is also influenced by a number of variables, including the isolated environment of the desired strain, material composition, particle size, and shape (Joshi et al., 2008). Furthermore, a lot of study has been done on the creation of SeNPs, which shows that the presence of SeNPs is indicated by distinct absorption peaks (Hemalatha et al., 2014).

Furthermore, studies show that several biomolecules or macromolecules, including proteins and polysaccharides, cover SeNPs produced by bacteria (Abou-Dobara et al., 2024; El-Dein et al., 2021; El-Zahed et al., 2021). Indeed, proteins and carbohydrates have the ability to reduce metal salts to metal NPs. Through the vibration of the functional groups (proteins and carbohydrates) of the nanoparticles, there are certain frequent issues with nanoparticle stability. Accumulation and aggregation of NPs are major issues that limit their utilization in various applications. Capping agents have a significant role in limiting NP aggregation. FT-IR analysis might yield valuable semiquantitative information regarding the existence of biological components in the coating layers of the nanoparticles and their related contents (Tugarova & Kamnev, 2017). The FT-IR study verified the presence of proteins as capping agents around the NPs. Some investigations confirm that protein capping compounds increase the stability of NPs via cysteine and amine residues, preventing NPs accumulation and aggregation (Escobar-Ramírez et al., 2021). In addition, the amide III band of proteins was discovered when using *pseudomonas sp* in the production of SeNPs. This capping agent may

contain negative or positive charges, which play a crucial role in NP stability and colloidal dispersion. SeNPs biosynthesized by *Penicillium* sp. were shown to have a negative charge of -11.8mV, creating a repulsion force between NP grains and increasing their stability. Laslo et al., (2022) found that *L. casei* produced SeNPs with a maximum zeta potential of -23 mV. It is worth noting that the zeta potential surface charge of NPs plays a significant role in antibacterial activity via electrostatic adhesion interactions with microbial cell membranes (Hnain et al., 2013). Our antibacterial activity data showed that SeNPs were effective against both Gram-positive and Gram-negative bacteria. Because Gram-positive and Gram-negative bacteria have different cell wall compositions. It was revealed that SeNPs showed a higher antibacterial activity against Gram-positive bacteria than Gram-negative. Thick walls and substantial levels of peptidoglycan discovered in Gram-positive bacteria's cell walls reduced the harmful impacts of these NPs when compared to Gram-negative bacteria. Several investigations have demonstrated SeNPs' bactericidal effects, which include the generation of reactive oxygen species, changes in cell wall permeability, and cell wall disintegration. SeNPs may interact with microbes' cell walls, triggering cell bursts, among other plausible explanations for their putative antimicrobial properties (Escobar-Ramírez et al., 2021).

The current work biosynthesized SeNPs using *P. aeruginosa* and investigated their antimicrobial activity. The antibacterial activity of SeNPs was tested against different Gram-positive bacteria, Gram-negative bacteria, and yeast in comparison to the standard antimicrobials ampicillin and miconazole using the agar well diffusion method, MIC, and MBC tests. Bacteria cannot multiply when an inhibition zone appears, proving that a treatment is working against them. Compared to SeNPs, *P. aeruginosa* and *P. mirabilis* displayed a complete resistance towards ampicillin. It was shown that SeNPs are more effective against bacteria that are Gram-positive than those that are Gram-negative. This is explained by a substantial change in the makeup of the bacterial walls. Numerous holes were discovered in the cell walls of Gram-positive bacteria, which facilitate the entry of NPs into the bacterial cells. This increases the NPs'

reactivity with bacterial components and fortifies their antibacterial action (Pasquina-Lemonche et al., 2020). In a similar way, biosynthesized SeNPs utilizing *Pseudomonas* sp. demonstrated greater biocidal effect against *C. albicans* with MIC and MFC values of 25 µg/ml than the conventional medication miconazole (40 µg/ml). El-Saadony et al. (2021) found an MIC and MFC of 55 and 80 µg/ml for SeNPs against *C. albicans*. Shakibaie et al. (2015) generated SeNPs using *Bacillus* species Msh1 and found a MIC of 70 µg/mL against *C. albicans*. Aside from the low MIC value of the biosynthesized SeNPs, the cytotoxic effect on normal keratinocyte cells was determined using the trypan blue method. SeNPs have a low hazardous effect, with an IC₅₀ of around 41.5 µg/mL.

Well-known antimicrobials, SeNPs mainly use oxidative stress to target bacteria. Reactive oxygen species (ROS) are produced, which causes the bacterial cell wall to break and release proteins and nucleic acids. ROS also causes significant respiratory enzymes to malfunction and oxidize important proteins like glutathione, which kills germs (Sahoo et al., 2023). The main mechanism by which Se NPs attack bacteria is oxidative stress. Proteins and nucleic acids are released when the bacterial cell wall breaks down due to the production of ROS. According to Sahoo et al. (2023), ROS also oxidizes important proteins like glutathione and causes critical respiratory enzymes to malfunction, killing bacteria. According to the acquired data, Se NPs demonstrated a concentration-dependent scavenging effect: the radical scavenging ratio rose as the concentrations in the tested range increased. Se NPs have a 68.2% DPPH radical scavenging activity. In this study, the conventional antioxidant ascorbic acid worked better than the Se NPs at all doses. Se NPs, which are efficient nanometallic compounds, improve cell permeability to NPs by destabilizing bacterial membranes and enhancing the biocidal action against the tested bacteria. SeNPs, which are effective nanometallic compounds, increase cell permeability to NPs by making bacterial membranes unstable. They have demonstrated a great deal of potential as a multipurpose antibiotic. The prospective use of SeNPs as promising single or combination antibacterial treatments in a range of environmental, industrial, and medical applications was

validated by these results.

Conclusions

The cell-free supernatant of the clinical isolate *P. aeruginosa* is used in this work to biosynthesize SeNPs in an easy and environmentally friendly manner. FT-IR was used to determine the presence of the bacterial proteins, which may serve as a reducing and stabilizing agent. FT-IR, zeta analysis, TEM, and UV-Vis spectroscopy were used to confirm the synthesis of SeNPs. The SeNPs' long-term stability was shown by their zeta potential and FT-IR measurement. With MIC values ranging from 45 to 150 µg/ml, the biosynthesized SeNPs demonstrated strong antibacterial and anticandidal properties against yeast and both Gram-positive and Gram-negative bacteria. Gram-positive bacteria were found to be more susceptible to SeNPs than Gram-negative bacteria, which may have uses in many pharmaceutical and medical applications, according to the results of the agar well diffusion assay, MIC, and MBC.

References:

- Abbas, H. S., Abou Baker, D. H., & Ahmed, E. A. (2021). Cytotoxicity and antimicrobial efficiency of selenium nanoparticles biosynthesized by *Spirulina platensis*. *Archives of Microbiology*, 203(2), 523–532. <https://doi.org/10.1007/s00203-020-02042-3>
- Abou-Dobara, M. I., Kamel, M. A., El-Sayed, A. K. A., & El-Zahed, M. M. (2024). Antibacterial activity of extracellular biosynthesized iron oxide nanoparticles against locally isolated β -lactamase-producing *Escherichia coli* from Egypt. *Discover Applied Sciences*, 6(3), 113. <https://doi.org/10.1007/s42452-024-05770-z>
- Atlas, R. M., & Snyder, J. W. (2011). Reagents, Stains, and Media: Bacteriology. In *Manual of Clinical Microbiology* (pp. 272–303). <https://doi.org/https://doi.org/10.1128/9781555816728.ch17>
- Baka, Z. A., El-sayed, A. K. A., & El-Zahed, M. M. (2019). Synthesis, characterization and antimicrobial activity of chitosan / Ag nanocomposite using *Escherichia coli* D8. *Scientific Journal for Damietta Faculty of Science*, 9(1), 1–6. <https://doi.org/10.21608/sjdfs.2019.194816>
- Besinis, A., Tracy, D. P., & and Handy, R. D. (2014). The antibacterial effects of silver, titanium dioxide and silica dioxide nanoparticles compared to the dental disinfectant chlorhexidine on *Streptococcus mutans* using a suite of bioassays. *Nanotoxicology*, 8(1), 1–16. <https://doi.org/10.3109/17435390.2012.742935>
- Clinical and Laboratory Standards (CLSI). (2000a). Performance standards for antimicrobial disk susceptibility tests, 7th ed. Approved standard M2–A7. National Committee for Clinical Laboratory Standards Wayne, Pa.
- CLSI. (2000b). Methods for dilution antimicrobial susceptibility test for bacteria that grow aerobically. Wayne, PA: *Clinical and Laboratory Standards Institute*.
- CLSI. (2008). Reference method for broth dilution antifungal susceptibility testing of yeasts; approved standard M27-A3. Wayne, PA: *Clinical and Laboratory Standards Institute*.
- CLSI. (2017). *Performance standards for antimicrobial susceptibility testing: Approved standard-twenty-seven edition* (Vols. M100-S26). Clinical and Laboratory Standards Institute, Wayne, Pennsylvania, USA.
- El-Deeb, B., Al-Talhi, A., Mostafa, N., & Abou-Assy, R. (2018). Biological synthesis and structural characterization of selenium nanoparticles and assessment of their antimicrobial properties. *American Scientific Research Journal for Engineering, Technology, and Sciences*, 45(1), 135–170.
- El-Dein, M. M. N., Baka, Z. A. M., Abou-Dobara, M. I., El-Sayed, A. K. A., & El-Zahed, M. M. (2021). Extracellular biosynthesis, optimization, characterization and antimicrobial potential of *Escherichia coli* D8 silver nanoparticles. *Journal of Microbiology, Biotechnology and Food Sciences*, 10(4), 648–656. <https://doi.org/10.15414/jmbfs.2021.10.4.648-656>
- El-Saadony, M. T., Saad, A. M., Taha, T. F., Najjar, A. A., Zabermawi, N. M., Nader, M. M., AbuQamar, S. F., El-Tarabily, K. A., & Salama, A. (2021). Selenium nanoparticles from *Lactobacillus paracasei* HM1 capable of antagonizing animal pathogenic fungi as a new source from human breast milk. *Saudi Journal of Biological Sciences*, 28(12), 6782–6794.
- El-Zahed, A. A. Z., Khalifa, M. E., El-Zahed, M. M., & Baka, Z. A. (2023). Biological synthesis and characterization of antibacterial manganese oxide nanoparticles using *Bacillus subtilis* ATCC6633. *Scientific Journal for Damietta Faculty of Science*, 13(3), 79–87. <https://doi.org/10.21608/sjdfs.2023.242279.1136>
- El-Zahed, M. M., Baka, Z., Abou-Dobara, M. I., & El-Sayed, A. (2021). *In vitro* biosynthesis and antimicrobial potential of biologically reduced

- graphene oxide/ag nanocomposite at room temperature. *Journal of Microbiology, Biotechnology and Food Sciences*, 10(6), e3956–e3956. <https://doi.org/10.15414/jmbfs.3956>
- Escobar-Ramírez, M. C., Castañeda-Ovando, A., Pérez-Escalante, E., Rodríguez-Serrano, G. M., Ramírez-Moreno, E., Quintero-Lira, A., Contreras-López, E., Añorve-Morga, J., Jaimez-Ordaz, J., & González-Olivares, L. G. (2021). Antimicrobial activity of Se-nanoparticles from bacterial biotransformation. *Fermentation*, 7(3), 130. <https://doi.org/https://doi.org/10.3390/fermentation7030130>
- Fayed, R., Elnemr, A.-M., & El-Zahed, M. M. (2023). Synthesis, characterization, antimicrobial and electrochemical studies of biosynthesized zinc oxide nanoparticles using the probiotic *Bacillus coagulans* (ATCC 7050). *Journal of Microbiology, Biotechnology and Food Sciences*, 13(3), e9962. <https://doi.org/10.55251/jmbfs.9962>
- Fesharaki, P. J., Nazari, P., Shakibaie, M., Rezaie, S., Banoee, M., Abdollahi, M., & Shahverdi, A. R. (2010). Biosynthesis of selenium nanoparticles using *Klebsiella pneumoniae* and their recovery by a simple sterilization process. *Brazilian Journal of Microbiology*, 41, 461–466. <https://doi.org/https://doi.org/10.1590/S1517-83822010000200028>
- Garg, P., Sharma, S., & Rao, G. N. (1999). Ciprofloxacin-resistant pseudomonas keratitis11The authors have no proprietary interest in any of the products mentioned in this article. *Ophthalmology*, 106(7), 1319–1323. [https://doi.org/https://doi.org/10.1016/S0161-6420\(99\)00717-4](https://doi.org/https://doi.org/10.1016/S0161-6420(99)00717-4)
- Gniadkowski, M. (2001). Evolution and epidemiology of extended-spectrum β -lactamases (ESBLs) and ESBL-producing microorganisms. *Clinical Microbiology and Infection*, 7(11), 597–608. <https://doi.org/https://doi.org/10.1046/j.1198-743x.2001.00330.x>
- Hemalatha, T., Krithiga, G., Santhosh Kumar, B., & Sastry, T. P. (2014). Preparation and characterization of hydroxyapatite-coated selenium nanoparticles and their interaction with osteosarcoma (SaOS-2) cells. *Acta Metallurgica Sinica (English Letters)*, 27, 1152–1158.
- Hnain, A., Brooks, J., & Lefebvre, D. D. (2013). The synthesis of elemental selenium particles by *Synechococcus leopoliensis*. *Applied Microbiology and Biotechnology*, 97(24), 10511–10519. <https://doi.org/10.1007/s00253-013-5304-0>
- Huh, A. J., & Kwon, Y. J. (2011). “Nanoantibiotics”: a new paradigm for treating infectious diseases using nanomaterials in the antibiotics resistant era. *Journal of Controlled Release*, 156(2), 128–145. <https://doi.org/https://doi.org/10.1016/j.jconrel.2011.07.002>
- Husseiny, M. I., Abd El-Aziz, M., Badr, Y., & Mahmoud, M. A. (2007). Biosynthesis of gold nanoparticles using *Pseudomonas aeruginosa*. *Spectrochimica Acta Part A: Molecular and Biomolecular Spectroscopy*, 67(3–4), 1003–1006. <https://doi.org/https://doi.org/10.1016/j.saa.2006.09.028>
- Iqtedar, M., Mehral, A., Muhammad, A., Asma, S., Roheena, A., & and Kaleem, A. (2019). Extracellular biosynthesis, characterization, optimization of silver nanoparticles (AgNPs) using *Bacillus mojavensis* BTCB15 and its antimicrobial activity against multidrug resistant pathogens. *Preparative Biochemistry & Biotechnology*, 49(2), 136–142. <https://doi.org/10.1080/10826068.2018.1550654>
- Joshi, M., Bhattacharyya, A., & Ali, S. W. (2008). Characterization techniques for nanotechnology applications in textiles. *Indian Journal of Fibre & Textile Research*, 33, 304–317. <https://www.scirp.org/reference/referencespapers?referenceid=1237990>
- Khan, Y., Sadia, H., Ali Shah, S. Z., Khan, M. N., Shah, A. A., Ullah, N., Ullah, M. F., Bibi, H., Bafakeeh, O. T., & Khedher, N. Ben. (2022). Classification, synthetic, and characterization approaches to nanoparticles, and their applications in various fields of nanotechnology: a review. *Catalysts*, 12(11), 1386. <https://doi.org/https://doi.org/10.3390/catal12111386>
- Khurana, A., Tekula, S., Saifi, M. A., Venkatesh, P., & Godugu, C. (2019). Therapeutic applications of selenium nanoparticles. *Biomedicine & Pharmacotherapy*, 111, 802–812. <https://doi.org/https://doi.org/10.1016/j.biopha.2018.12.146>
- Kunz Coyne, A. J., El Ghali, A., Holger, D., Rebold, N., & Rybak, M. J. (2022). Therapeutic strategies for emerging multidrug-resistant *Pseudomonas aeruginosa*. *Infectious Diseases and Therapy*, 11(2), 661–682. <https://doi.org/10.1007/s40121-022-00591-2>
- Laslo, V., Pinzaru, S. C., Zagula, G., Kluz, M., Vicas, S. I., & Cavalu, S. (2022). Synergic effect of selenium nanoparticles and lactic acid bacteria in reduction cadmium toxicity. *Journal of Molecular Structure*, 1247, 131325. <http://dx.doi.org/10.1016/j.molstruc.2021.131325>
- Manimaran, M., Muthuvel, A., & Said, N. M. (2023). Microwave-assisted green synthesis of

- SnO₂ nanoparticles and their photocatalytic degradation and antibacterial activities. *Nanotechnology for Environmental Engineering*, 8(2), 413–423. <https://doi.org/10.1007/s41204-022-00297-3>
- Miller, W. R., & Arias, C. A. (2024). ESKAPE pathogens: Antimicrobial resistance, epidemiology, clinical impact and therapeutics. *Nature Reviews Microbiology*, 22(10), 598–616. <https://doi.org/10.1038/s41579-024-01054-w>
- Mohamed, E. A., & El-Zahed, M. M. (2024). Anticandidal applications of selenium nanoparticles biosynthesized with *Limosilactobacillus fermentum* (OR553490). *Discover Nano*, 19(1), 115. <https://doi.org/10.1186/s11671-024-04055-z>
- Moore, D. F., Hamada, S. S., Marso, E., & Martin, W. J. (1981). Rapid identification and antimicrobial susceptibility testing of Gram-negative bacilli from blood cultures by the AutoMicrobic system. *Journal of Clinical Microbiology*, 13(5), 934–939. <https://doi.org/10.1128/jcm.13.5.934-939.1981>
- Murray, C. J. L., Ikuta, K. S., Sharara, F., Swetschinski, L., Aguilar, G. R., Gray, A., Han, C., Bisignano, C., Rao, P., & Wool, E. (2022). Global burden of bacterial antimicrobial resistance in 2019: A systematic analysis. *The Lancet*, 399(10325), 629–655. [https://doi.org/10.1016/S0140-6736\(21\)02724-0](https://doi.org/10.1016/S0140-6736(21)02724-0)
- O'Neill, J. (2016). *Tackling drug-resistant infections globally: final report and recommendations*. Available online at: <https://www.cabidigitallibrary.org/doi/full/10.5555/20173071720>
- Owuama, C. I. (2017). Determination of minimum inhibitory concentration (MIC) and minimum bactericidal concentration (MBC) using a novel dilution tube method. *African Journal of Microbiology Research*, 11(23), 977–980. <https://doi.org/10.5897/AJMR2017.8545>
- Parte, A. C., Sardà Carbasse, J., Meier-Kolthoff, J. P., Reimer, L. C., & Göker, M. (2020). List of prokaryotic names with standing in nomenclature (LPSN) moves to the DSMZ. *International Journal of Systematic and Evolutionary Microbiology*, 70(11), 5607–5612. <https://doi.org/https://doi.org/10.1099/ijsem.0.004332>
- Poku, E., Cooper, K., Cantrell, A., Harnan, S., Sin, M. A., Zanzudana, A., & Hoffmann, A. (2023). Systematic review of time lag between antibiotic use and rise of resistant pathogens among hospitalized adults in Europe. *JAC-Antimicrobial Resistance*, 5(1), dlad001. <https://doi.org/https://doi.org/10.1093/jacamr/dlad001>
- Reygaert, W. C. (2018). An overview of the antimicrobial resistance mechanisms of bacteria. *AIMS Microbiology*, 4(3), 482. <https://doi.org/10.3934/microbiol.2018.3.482>
- Sahoo, B., Leena Panigrahi, L., Jena, S., Jha, S., & Arakha, M. (2023). Oxidative stress generated due to photocatalytic activity of biosynthesized selenium nanoparticles triggers cytoplasmic leakage leading to bacterial cell death. *RSC Advances*, 13(17), 11406–11414. <https://doi.org/10.1039/D2RA07827A>
- Santiago-Rodriguez, T. M., Ly, M., Bonilla, N., & Pride, D. T. (2015). The human urine virome in association with urinary tract infections. *Frontiers in Microbiology*, 6, 14. <https://www.frontiersin.org/journals/microbiology/articles/10.3389/fmicb.2015.00014>
- Saqib, S., Nazeer, A., Ali, M., Zaman, W., Younas, M., Shahzad, A., Sunera, & Nisar, M. (2022). Catalytic potential of endophytes facilitates synthesis of biometallic zinc oxide nanoparticles for agricultural application. *BioMetals*, 35(5), 967–985. <https://doi.org/10.1007/s10534-022-00417-1>
- Shakibaie, M., Mohazab, N. S., & Mousavi, S. A. A. (2015). Antifungal activity of selenium nanoparticles synthesized by *Bacillus* species Msh-1 against *Aspergillus fumigatus* and *Candida albicans*. *Jundishapur Journal of Microbiology*, 8(9), e26381. <https://doi.org/10.5812/jjm.26381>
- Srivastava, N., & Mukhopadhyay, M. (2015). Green synthesis and structural characterization of selenium nanoparticles and assessment of their antimicrobial property. *Bioprocess and Biosystems Engineering*, 38(9), 1723–1730. <https://doi.org/10.1007/s00449-015-1413-8>
- Subedi, D., Ajay Kumar, V., & Willcox, M. (2018). Overview of mechanisms of antibiotic resistance in *Pseudomonas aeruginosa*: An ocular perspective. *Clinical and Experimental Optometry*, 101(2), 162–171. <https://doi.org/10.1111/cxo.12621>
- Tabibi, M., Ageai, S. S., Amoozegar, M. A., Nazari, R., & Zolfaghari, M. R. (2020). Antibacterial, antioxidant, and anticancer activities of biosynthesized selenium nanoparticles using two indigenous halophilic bacteria. *Archives of Hygiene Sciences*, 9(4), 275–286. <http://dx.doi.org/10.52547/ArchHygSci.9.4.275>
- Tugarova, A. V., & Kamnev, A. A. (2017). Proteins in microbial synthesis of selenium nanoparticles. *Talanta*, 174, 539–547. <https://doi.org/https://doi.org/10.1016/j.talanta.2017.06.013>
- Turan, N., Kızılkaya, S., Buldurun, K., Çolak, N., Akdeniz, A., & Bursal, E. (2025). Synthesis, enzyme inhibitory and antioxidant activities, and molecular docking studies of metal complexes of

- a Schiff base ligand bearing pyridine moiety. *Journal of Molecular Structure*, 1338, 142167. <https://doi.org/https://doi.org/10.1016/j.molstruc.2025.142167>
- Wang, L., Chen, H., & and Shao, L. (2017). The antimicrobial activity of nanoparticles: present situation and prospects for the future. *International Journal of Nanomedicine*, 12(null), 1227–1249. <https://doi.org/10.2147/IJN.S121956>
- Xiao, D., Chao, X., Chunyan, Y., Peiyi, Y., Hongjian, Y., Qunying, G., Fengxian, H., Yao-Zhong, K., & Xiao, Y. (2024). Clinical characteristics and antibiotic treatment of peritoneal dialysis-associated peritonitis caused by *Pseudomonas* species: a review of 15 years' experience from southern China. *Microbiology Spectrum*, 12(6), e00096-24. <https://doi.org/10.1128/spectrum.00096-24>
- Yahr, T. L., & Parsek, M. R. (2006). *Pseudomonas aeruginosa*. In M. Dworkin, S. Falkow, E. Rosenberg, K.-H. Schleifer, & E. Stackebrandt (Eds.), *The Prokaryotes: A Handbook on the Biology of Bacteria Volume 6: Proteobacteria: Gamma Subclass* (pp. 704–713). Springer New York. https://doi.org/10.1007/0-387-30746-X_22
- Youri, G., Catherine, B., Caroline, B., & Pierre, B. (2007). Evaluation of a new selective chromogenic agar medium for detection of extended-spectrum β -lactamase-producing Enterobacteriaceae. *Journal of Clinical Microbiology*, 45(2), 501–505. <https://doi.org/10.1128/jcm.02221-06>
- Zboromyrska, Y., & Vila, J. (2016). Advanced PCR-based molecular diagnosis of gastrointestinal infections: Challenges and opportunities. *Expert Review of Molecular Diagnostics*, 16(6), 631–640. <https://doi.org/10.1586/14737159.2016.1167599>

الملخص العربي

عنوان البحث: النشاط المضاد ميكروبي لجسيمات السيلينيوم النانومترية المصنعة حيويًا باستخدام عزلة سيدوموناس إيروجينوزا

ليلى عبد السميع الشخبيي^١، زكريا عوض محمد بقا^١، محمد مرزوق الزاهد^{١*}

^١ قسم النبات والميكروبيولوجي، كلية العلوم، جامعة دمياط، دمياط الجديدة، مصر

استخدمت الدراسة الحالية بكتيريا سيدوموناس إيروجينوزا المعزولة من بعض العينات الطبية في التصنيع الحيوي لتصنيع جسيمات السيلينيوم النانومترية باستخدام نهج بسيط وفعال وقليل التكلفة. وقد استخدم جهاز Vitek 2 لتأكيد تحديد مستوى النوع للعزلة البكتيرية المختارة بعد التعرف عليها بالطرق التقليدية. تم التحقق من إنتاج جسيمات السيلينيوم النانومترية المصنعة حيويًا ووصفها باستخدام مجموعة متنوعة من الاختبارات، بما في ذلك المجهر الإلكتروني النافذ، وتحليل الأشعة تحت الحمراء، وتحليل زيتا، والتحليل الطيفي للأشعة فوق البنفسجية المرئية. وقد سُجِلَت قمم الامتصاص لجسيمات السيلينيوم النانومترية عند موجة طولها ٣٣٠-٣٧٠ نانومتر، كما تم التحقق من وجود بروتينات بواسطة أطيف الأشعة تحت الحمراء والتي قد تعمل كمكونات رابطة وداعمة أثناء التصنيع الحيوي. وقد تم رصد شحنة سطحية سالبة كبيرة على أسطح الجسيمات والتي تصل إلى -١٧.٦ مللي فولت مما قد تساهم أيضًا في استقرارها. وقد أظهر المجهر الإلكتروني النافذ أقطار جسيمات السيلينيوم النانومترية في نطاق تراوح بين ٨٣-٩١ نانومتر. كما أظهرت جسيمات السيلينيوم النانومترية نشاطًا قويًا ضد بكتيريا باسيلس سيريس، وستافيلوكوكس أوريوس، وسيدوموناس إيروجينوزا، وبروتئوس ميرابيليس، بالإضافة إلى خميرة كانديدا البيكانس، وذلك وفقًا للجرعة. وبلغت التركيزات المثبطة الدنيا لجسيمات السيلينيوم النانومترية ضد باسيلس سيريس، وستافيلوكوكس أوريوس، وسيدوموناس إيروجينوزا، وبروتئوس ميرابيليس، وخميرة كانديدا البيكانس ٤٠، و٧٠، و١١٠، و١٥٠، و١٥٠ ميكروجرام/مل، على التوالي. تقدم هذه الدراسة جسيمات نانومترية آمنة وفعالة وواعدة كبديل لعلاج بعض الميكروبات المسببة للأمراض لدى البشر والحيوانات.